About the Double-Humped Electron Distribution Function in Hall Thrusters

S. Barral, Z. Peradzyński, K. Makowski
Institute of Fundamental Technological Research
Świętokrzyska 21, 00049 Warsaw, Poland
e-mail: sbarral@ippt.gov.pl, kmak@ippt.gov.pl, zperadz@ippt.gov.pl

M. Dudeck
CNRS Laboratoire d'Aérothermique
1c avenue de la Recherche Scientifique, 45071 Orléans, France
e-mail: dudeck@cnrs-orleans.fr

IEPC-01-25

There is currently no unanimous consensus on the shape and interpretation of the electron energy distribution function in a Hall Thruster, but many experimental evidences have been accumulated which suggest that this distribution is characterized by at least two maxima. Theoretical as well as numerical studies have recently comforted this theory, but have not given much insight about the origins of the second maximum, nor about the influence of external parameters on the distribution. A phenomenological explanation of the possible double-hump of the energy distribution function is given, based on the probability density of energy of electrons involved in a cyclotron motion. A theoretical model proposed by other authors [1] is investigated by the mean of Monte-Carlo simulation, extending the original model to the case of collision-driven transport. The effect of elastic collisions is shown to be relatively modest and not to disturb significantly the distribution, but a detailed study of inelastic processes suggests that the dispersion of velocities after dissipative collisions is too large to induce a significant high energy hump in the distribution.

1 Introduction

The electron energy distribution function (EEDF) measured experimentally in Hall thrusters invariably exhibits two or three peaks [2, 3, 4]. The peculiar shape of the EEDF was given different interpretations, generally involving the presence of several populations of electrons associated with distinct processes, such as ionization or secondary emission at the walls [4].

Some numerical studies have also shown that in some circumstances a high energy peak may appear, although it could not be clearly associated with a given physical process [5, 6, 7]. With a different approach, Fedotov *et al*. [1] have given a theoretical evidence that a single population can account for two energy maximum when involved in a $E \times B$ drift, provided that thermal relaxation is weak.

The following work intends to cross the bridge between these two approaches through a confrontation of the theoretical results with a simple particle model, in order to define more precisely the meaning and the applicability of the EEDF given in [1]. The aforementioned theoretical distribution corresponds to the EEDF in a low density plasma dominated by inelastic collisions, which is consistent with the characteristic of the discharge in Hall thrusters in the high magnetic field region. It will be shown, however, that the estimation of the dispersion in electron velocity after inelastic collisions is critical for the computation of the EEDF and cannot be achieved without a more detailed analysis of collision processes. The simple theoretical model is for this reason extended in the frame of a Monte-Carlo simulation to account for the effect of elastic collisions, ionization, excitations and collisions with the walls.

2 Preliminary discussion

2.1 Probability density of state of a single electron

The presence of two energy maxima in the EEDF of an unrelaxed electron population submitted to the influence of perpendicular $\overrightarrow{E}$ and $\overrightarrow{B}$ fields can be simply explained by observing the motion of a single electron.

Let us name $v_\parallel$, v_φ and v_z the coordinates of the velocity vector in the direction of $\overrightarrow{B}$, of the drift and of $\overrightarrow{E}$ respectively. The energy of a single electron describing the well-known cycloidal motion and its time derivative in Lagrangian coordinates are given by:

$$\begin{aligned}\varepsilon(t) = \frac{1}{2}m_e\left[v_{\parallel 0}^2 + (v_{\varphi 0} - u_d)^2 + v_{z0}^2 + u_d^2\right] \\ + m_e u_d\sqrt{(v_{\varphi 0} - u_d)^2 + v_{z0}^2}\,\sin(\omega_B t + \psi_0)\end{aligned} \tag{1}$$

$$\dot{\varepsilon}(t) = m_e\omega_B u_d\sqrt{(v_{\varphi 0} - u_d)^2 + v_{z0}^2}\cos(\omega_B t + \psi_0) \tag{2}$$

where $u_d = \frac{E}{B}$ stands for the drift velocity , m_e for the mass of an electron, ω_B for the electron cyclotron frequency and ψ_0 for the initial phase of the particle in the (φ, z) plane and in the referential of the drift:

$$\tan\psi_0 = \frac{v_\varphi - u_d}{v_z}$$

The stationary Liouville equation for the energy probability density of a single electron $\mathcal{D}_e$ reads:

$$\frac{d\left(\mathcal{D}_e\dot{\varepsilon}\right)}{d\varepsilon} = 0 \tag{3}$$

which can be integrated to obtain the expression of the normalized probability density:

$$\begin{cases} \mathcal{D}_e(\varepsilon) = \dfrac{1}{\pi\sqrt{\varepsilon - \varepsilon_{min}}\sqrt{\varepsilon_{max} - \varepsilon}} & \varepsilon \in [\varepsilon_{min}, \varepsilon_{max}] \\ \mathcal{D}_e(\varepsilon) = 0 & \varepsilon \notin [\varepsilon_{min}, \varepsilon_{max}] \end{cases} \tag{4}$$

with:

$$\begin{aligned}\varepsilon_{min} &= \frac{1}{2}m_e\left[u_d - \sqrt{(v_{\varphi 0} - u_d)^2 + v_{z0}^2}\right]^2 + \frac{1}{2}m_e v_{\parallel 0}^2 \\ \varepsilon_{max} &= \frac{1}{2}m_e\left[u_d + \sqrt{(v_{\varphi 0} - u_d)^2 + v_{z0}^2}\right]^2 + \frac{1}{2}m_e v_{\parallel 0}^2\end{aligned} \tag{5}$$

The probability density $\mathcal{D}_e$ exhibits two peaks of infinite height located at ε_{min} and ε_{max} which are associated with longer transit time in the high and low energy portions of the trajectory than in the intermediate energy portion, as illustrated by Fig.1.

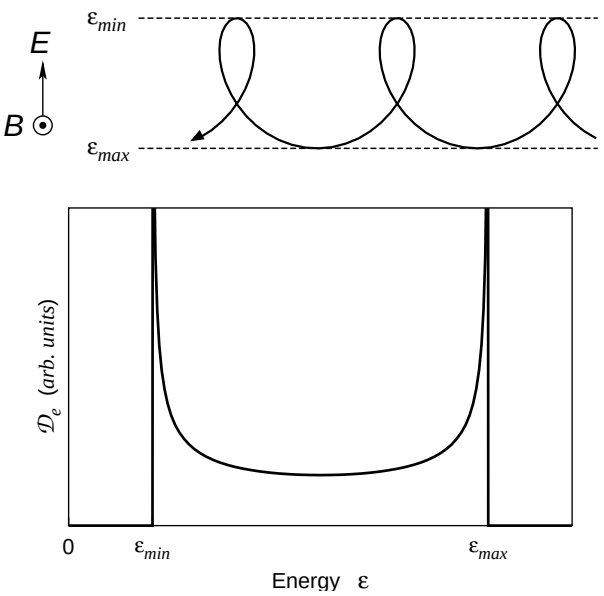

Figure 1: Position of energy extrema in the trajectory of an electron submitted to $\overrightarrow{E} \times \overrightarrow{B}$ fields and corresponding energy probability density

This probability density can be understood as the contribution of every single electron to the overall distribution function of a collisionless electron medium. If for instance all electrons were born with zero energy and were involved in a infinite motion, the (normalized) distribution function of this homogeneous collisionless plasma would exactly coincide with the probability density of state $\mathcal{D}_e$ corresponding to $\varepsilon_{min} = 0$ and $\varepsilon_{max} = 2m_e u_d^2$.

2.2 Collisionless electron medium

A more complex case was studied in [1] where some dispersion on the initial velocity dispersion of electrons was accounted for in a qualitative way by taking the initial velocity distribution of electrons (i.e. the undisturbed velocity distribution of electrons before they are submitted to the $\overrightarrow{E} \times \overrightarrow{B}$ fields) as Maxwellian at a temperature T_p. Although the approach taken by the authors to obtain the resulting EEDF was based on integrals of motions, one could formally express the normalized en-

ergy distribution $\mathcal{F}$ of this electron medium as follows:

$$\mathcal{F}(\varepsilon) = \int\int\int dv_{\parallel 0}\, dv_{\varphi 0}\, dv_{z0} \times f_{\mathcal{M}}(v_{\parallel 0}, v_{\varphi 0}, v_{z0}) \times \mathcal{D}_e\left[\varepsilon, \varepsilon_{min}(u_d, v_{\parallel 0}, v_{\varphi 0}, v_{z0}), \varepsilon_{max}(u_d, v_{\parallel 0}, v_{\varphi 0}, v_{z0})\right] \quad (6)$$

where $f_{\mathcal{M}}$ is a normalized Maxwellian velocity distribution.

An expression of this EEDF in term of a simple integral was given by Fedotov *et al.*[*]:

$$\mathcal{F}(\varepsilon) = \frac{e^{-\frac{\varepsilon}{T_p}}}{\pi^{\frac{3}{2}}\sqrt{\varepsilon_d T_p}} \int_0^{\frac{\pi}{2}} d\Psi \times \frac{e^{-4\frac{\varepsilon_d}{T_p}\sin^2\Psi}}{\sin\Psi} \sinh\left(4\frac{\sqrt{\varepsilon\cdot\varepsilon_d}}{T_p}\sin\Psi\right) \quad (7)$$

where $\varepsilon_d = \frac{1}{2}m_e u_d^2$ is the drift energy.

The shape of this distribution for different ratios $\frac{T_p}{\varepsilon_d}$ is given on Fig.2 which shows clearly the similarity between $\mathcal{F}$ at $T_p = 0$ and $\mathcal{D}_e$. It can be seen that the second extremum disappears if the initial dispersion in velocities is too large. It can be verified that in the limit $\frac{T_p}{\varepsilon_d}\to\infty$ the distribution $\mathcal{F}$ tends to a Maxwellian distribution, which simply means that as the effect of magnetization is canceled the initial distribution is recovered.

2.3 The electron beam

The presence of a beam of electrons emitted by the cathode was a main concern in the theoretical work mentioned above [1]. Although we do not discard such a possibility, the suggestion that the associated EEDF could exhibit a double hump seem debatable. Indeed, when computing the EEDF by integration of the cyclotron motion of electrons as it was done in the previous section, one implicitly makes the assumption that the plasma is uniform since this approach is formally equivalent to integrating the EEDF over the volume in which electrons evolve. This assumption is not valid for an electron beam which acquires energy as it travels towards anode without dissipating it.

We believe that in the case of an electron beam, the double-humped distribution is an artifact of the integration over the cyclotron trajectory that does not correspond to a tangible physical effect. Since in our understanding electrons belonging to the beam are transported via elastic collisions, the EEDF at a given point should be simply equal to the initial EEDF at cathode shifted by the potential drop between cathode and the point considered since the energy acquired is conserved and is the same for all electrons.

[*] the present expression is drawn from an erratum relative to the original publication issued by the authors to N. B. Meezan

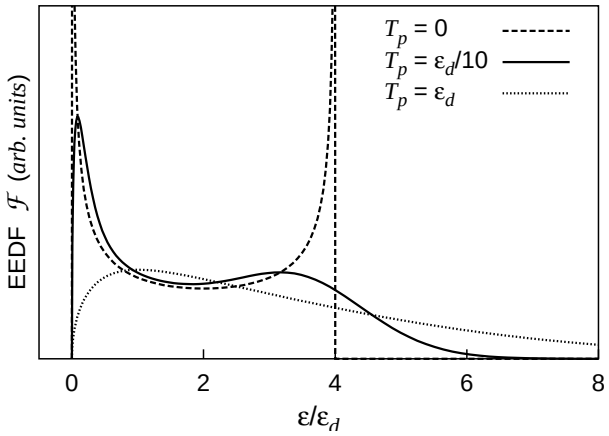

Figure 2: Shape of the energy distribution function $\mathcal{F}$ for different ratios $\frac{T_p}{\varepsilon_d}$.

3 Idealized collision model

3.1 Numerical model

A classical Monte-Carlo method is used to simulate electron transport within the frame of the planar approximation, assuming that the plasma is uniform in space. This last assumption is justified by the strong confinement of electrons induced by the B field which leads to a near-local adjustment of the energy distribution function as a function of the plasma parameters and electromagnetic fields. A similar argument was independently proposed by other authors [8] for the study of the EEDF in a Hall thruster, citing an earlier study of the EEDF in a magnetron [9]. Besides, a local energy balance approximation was successfully used and justified for the computation of electron temperature in a 1D Hall thruster simulation [10].

A single electron is introduced in the cross-fields, and its velocity vector is subsequently tracked in all three dimensions. The initial state of the electron is meaningless since stochastic collisions quickly remove any correlation between current and initial states (in practice, some

3-4 collisions are enough to "forget" about the initial state). This approach is somewhat related to the discussion of section 2.1, since it reposes one the idea that the EEDF results from the probability density of energy state of each electron. As it was previously pointed out, this approach is strictly valid only for a uniform plasma, and is justified here by the fact that the local energy balance inside the channel leads to reasonably low axial variations of the plasma properties on the scale of the cyclotron radius.

Analytical formulae are used to describe the evolution of electrons between consecutive energy levels of the discretized EEDF in order to eliminate possible discretization errors arising from the integration of trajectories.

3.2 Test-case with idealized inelastic collisions

3.2.1 Motivation

Although electron/electron collisions are indeed negligible in the channel of a Hall thruster, the collisionless approach mentioned in previous sections is of course somewhat artificial since the transport of electrons through the channel is heavily dependent on collision between electrons and other species (neutrals, ions, walls). It is therefore interesting to investigate the relevance of the collisionless distribution $\mathcal{F}$ in the presence of collisions. A comparison of the numerical model with $\mathcal{F}$ shall also confirm the validity of the numerical model.

3.2.2 Physical interpretation of $\mathcal{F}$ in the presence of inelastic collisions

Let us first clarify the meaning of the plasma temperature T_p introduced in section 2.2. This temperature is *not* what is usually defined as the temperature of electrons (written T_e in this study). The temperature T_p is a "background" temperature which gives an estimation of the velocity dispersion due to collisions, independently from the dispersion in velocities induced by the cyclotron motion. Indeed, the average energy of electrons for the distribution $\mathcal{F}$ is given by:

$$\overline{\varepsilon} = \frac{3}{2}T_p + 2\varepsilon_d$$

while the quantity usually denoted as electron temperature is by definition such that:

$$\overline{\varepsilon} = \frac{3}{2}T_e + \varepsilon_d$$

since the quantity $\frac{3}{2}T_e$ also accounts for the non-directed part of energy related to the cyclotron motion (equal to ε_d). Obviously, in a more exact treatment one should distinguish three quantities $T_{e\,\parallel} = T_p$, $T_{e\,\varphi} = T_p + \varepsilon_d$ and $T_{e\,z} = T_p + \varepsilon_d$ for each degree of freedom.

One may say therefore that the distribution $\mathcal{F}$ implicitly accounts for inelastic collisions, with the assumption that after inelastic collisions electrons are reemitted with velocity components $v_\parallel$, v_φ and v_z distributed according to a Gaussian law characterized by a standard-deviation $\sqrt{T_p/m_e}$.

It is also important to keep in mind that $\mathcal{F}$ was derived assuming that all electrons have the same weight in the overall distribution function, implying that the mean free flight time of electrons is independent from their initial velocity (indeed, the contribution of a single electron to the distribution function is proportional to its free flight time).

Finally, the contribution of each electron to the distribution $\mathcal{F}$ is determined from the probability density of state over an integer number of cyclotron rotations (this is an implicit assumption in the derivation of $\mathcal{D}_e$). This simplification is well justified for Hall thrusters where electrons typically perform many rotations between subsequent collisions due to relative order of magnitude between cyclotron and collision frequency ($\omega_B \gg \nu_{coll}$), and the probability density of state is therefore not strongly affected by the fact that electrons do not in general perform an integer number of rotations.

3.2.3 Model of collisions

On the basis of the discussion given above, only inelastic collisions were taken into account in this test-case and an idealized collision model consistent with the hypothesis made in the derivation of $\mathcal{F}$ was used.

The probability for an electron emitted at $t_0 = 0$ to collide with an neutral particle within a time interval $[0, t^*]$ is given by:

$$P_{coll}(t^*) = 1 - e^{-\frac{1}{N_a}\int_0^{t^*} \sigma_i(\varepsilon)\sqrt{\frac{2\varepsilon}{m_e}}\cdot dt} \qquad (8)$$

where σ_i is the inelastic collision cross-section and N_a the density of neutrals.

In order to stay close from the hypothesis made in deriving $\mathcal{F}$, the free flight time is made independent from the velocity of electrons by observing that in Eq. 8 the time t^* becomes uncorrelated with the velocity (or energy) if collision cross-sections vary according to:

$$\sigma_i^{ideal} = \frac{\alpha}{\sqrt{\varepsilon}} \qquad (9)$$

where α is a constant coefficient whose value is without incidence on the results as long as the condition $\omega_B \gg \nu_{coll}$ is satisfied.

The probability density of re-emission after an inelastic collision is given for each of the velocity component $v_\parallel$, v_φ and v_z by the aforementioned Gaussian law:

$$p_{v_i} = \sqrt{\frac{m_e}{2\pi \cdot T_p}} e^{-\frac{m_e v_i^2}{2T_p}} \tag{10}$$

Additional details on the stochastic model for collisions are deferred to section 4.1.

3.2.4 Results

The simulation was performed using typical parameters for the near-exit region of the channel of Hall thrusters:

- Electric field: $E = 40 \times 10^3\ V \cdot m^{-1}$
- Magnetic field: $B = 18\ mT$
- Density of neutrals: $N_a = 10^{18}\ m^{-3}$

It is difficult to estimate the background temperature T_p without resorting to a more detailed model as will be done later. Simulations were therefore performed for the cases studied earlier, namely $T_p = \frac{\varepsilon_d}{10}$ and $T_p = \varepsilon_d$ corresponding respectively to $T_p \approx 1.40\ eV$ and $T_p \approx 14.0\ eV$.

The coefficient α of Eq. 9 was taken equal to $10^{-19}\ m^2 eV^{-\frac{1}{2}}$. This cross-section variation law is of course very artificial, and one may legitimately wonder whether this assumption can lead to meaningful results. For this reason, other cases were studied where the cross-section were either taken constant:

$$\sigma_i^{const} = const = 10^{-20}\ m^2$$

or according to a "realistic" profile (denoted σ_i^{real}) corresponding to experimental ionization cross-sections for xenon [11].

The results are displayed on Fig. 3. The distribution $\mathcal{F}$ for $T_p = \frac{\varepsilon_d}{10}$ and $T_p = \varepsilon_d$ was given on Fig. 2 and is not reproduced here since it coincides exactly with the results obtained for cross sections σ_i^{ideal} (notwithstanding the random noise due to the computational method).

3.2.5 Discussion

The correlation between the theoretical results given by $\mathcal{F}$ and the computational results with "ideal" cross-sections σ_i^{ideal} supports the physical interpretation of $\mathcal{F}$ proposed in section 3.2.2 and simultaneously confirms the validity of the numerical model.

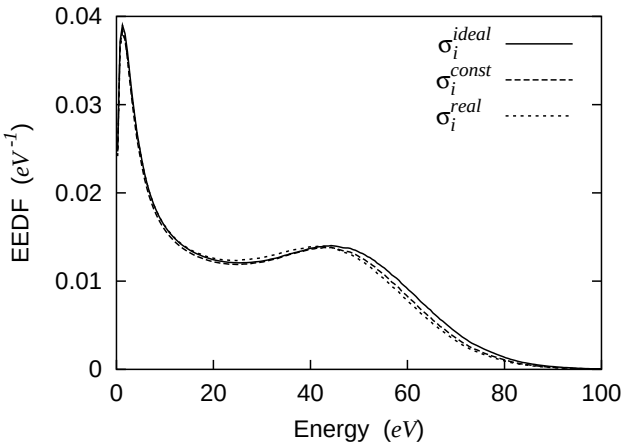

(a)

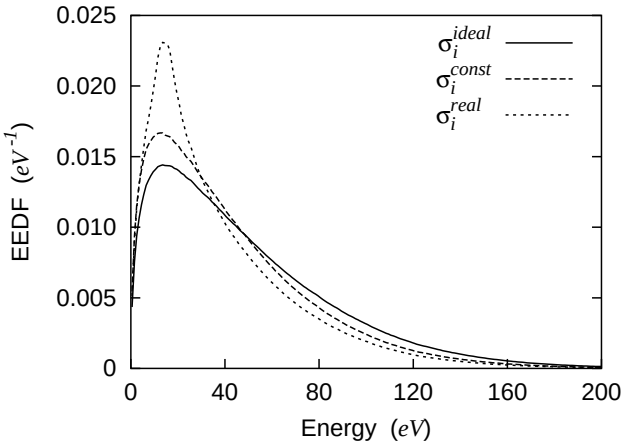

(b)

Figure 3: Computed EEDF with an idealized collision model accounting only for inelastic collisions for (a) $T_p = 1.4eV$ and (b) $T_p = 14eV$

As could be noticed earlier in section 2.2, the appearance of a double-humped distribution is mainly conditioned by the value of the ratio T_p/ε_d. This is easily understood physically since the dispersion in initial velocity after collision induces a dispersion on the location of the energy extrema ε_{min} and ε_{max} in the cyclotron trajectory between collisions which affects the sharpness of the peaks in the global EEDF.

It is interesting to note that the profile of cross-

sections has a very limited effect on the EEDF when $T_p = \varepsilon_d/10$. Indeed, since electrons perform many rotations between subsequent collisions, the free flight time is mainly determined by the probability density of energy over the cyclotron motion i.e. by ε_{min} and ε_{max}, and not directly by the initial velocity vector after collision. The parameters ε_{min} and ε_{max} do actually depend on the initial velocity vector, but as shown by Eq. 5 this dependence is very weak in the case $T_p \ll \varepsilon_d$.

One should also mention that the order of magnitude of the inelastic cross-sections has no effect here as long as the condition $\omega_B \gg \nu_{coll}$ is satisfied, since no other type of collisions (elastic scattering, wall collisions) was introduced at this point.

3.3 Effect of elastic collisions

Elastic scattering plays an important role in the relaxation of the plasma. In the acceleration zone of a Hall thrusters, elastic and inelastic collision frequencies are of the same order and it is therefore not possible to fully neglect elastic collisions.

The idealized model of inelastic collisions previously described was kept back in the present computations, using the "realistic" inelastic collision cross-sections σ_i^{real} and the elastic collision cross-sections of xenon from [12]. Excitation collisions were neglected since we make no attempt at this point to describe accurately all collision processes.

Results are displayed on figure 4 and show that as expected elastic collisions tend to thermalize the electron gas, but are not frequent enough to smooth out the high energy hump in the case of a low background temperature. A significant high energy tail can be observed, which behaves much like the high energy tail of a Maxwellian distribution with a decay in $\sqrt{\varepsilon}\, e^{-\varepsilon/T_0}$. Note that in the case of a low background temperature, the high energy tail could be correlated with the tail of a Maxwellian distribution whose total energy is higher than the actual EEDF, which must probably be attributed to the fact that the high energy hump is significant, hence a large incident energy before collision (high energy electrons prevail in the formation of the high energy tail since the probability of collision is higher for fast electrons than for slow electrons).

3.4 A brief summary

The main goal of the study led in this section was to assess the ability of the theoretical distribution (noted $\mathcal{F}$) to correctly describe the EEDF in the presence of elastic and inelastic collisions.

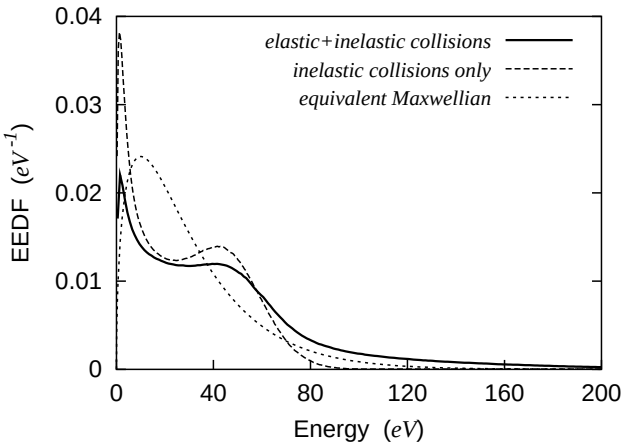

(a)

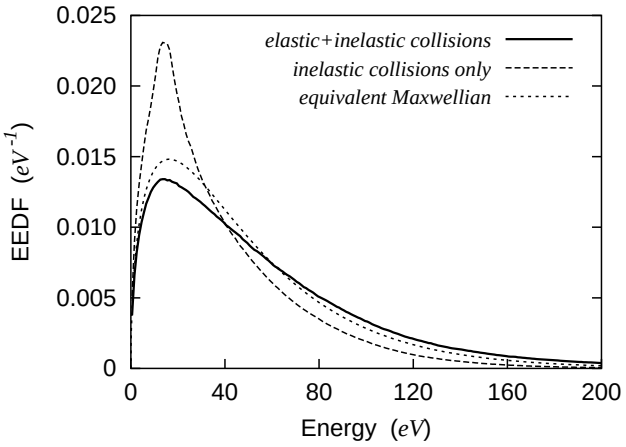

(b)

Figure 4: Computed EEDF with an idealized collision model accounting for elastic and inelastic collisions for (a) $T_p = 1.4eV$ and (b) $T_p = 14eV$. A Maxwellian distribution characterized by the same total energy is displayed for comparison

This results of simulations suggest that the qualitative shape of the EEDF can be reasonably described by the theoretical distribution even for realistic collision cross-sections and/or in the presence of elastic collisions, assuming that their magnitude is comparable to that of inelastic collisions, which is the case in the acceleration region of Hall thrusters.

The main shortcoming of this approach is its reliance

on a prescribed value of the dispersion of velocities caused by inelastic collisions (synthesized by the background temperature T_p). Unfortunately, the background temperature is not equivalent to the electron temperature and it is therefore not possible to rely on experimental measurements to estimate its value.

4 Real case study

4.1 Description of physical processes

In order to describe in a self-consistent manner the effect of velocity dispersion after inelastic collisions, the following collision model was used.

The phenomena taken into account are:

1. simple ionization
2. excitation (through a synthetic excitation level)
3. elastic scattering by neutrals
4. secondary emission/attachment at the walls and reflection on the sheath

For the sake of simplicity, it was assumed that the direction of re-emission after bulk collisions (ionization, excitation, elastic scattering) is statistically isotropic and uncorrelated with the direction of the incident electron, which leads to the following density probabilities for the deviation angle α and the angle of azimuth Ψ:

$$\begin{aligned} p_\alpha &= \frac{1}{2}\sin\alpha \quad & \alpha &\in [0,\pi] \\ p_\Psi &= \frac{1}{2\pi} & \Psi &\in [-\pi,\pi) \end{aligned}$$

The energy remaining after an ionization event is shared equally between primary and secondary electrons.

Since the excitation potentials of the most significant excitation levels of Xenon lie within a quite narrow range ($8.32 - 9.81\,eV$), these levels are grouped into a synthetic virtual excitation level of potential $9.2\,eV$ whose corresponding cross-section profile is computed from the sum of all excitation cross-sections (from [13]). It is important to note that only excitation and ionization from ground state are considered. Metastable levels are not distinguished from others and radiative processes are not included in the model, so that losses by excitation are probably overestimated.

Electrons hitting the sheath with a radial energy lower than the sheath potential are scattered elastically in a specular way. Electrons reaching the walls are either attached or scattered back into the plasma. One should in principle distinguish between backscattered electrons which are emitted with an energy comparable to the incident energy and true secondary electrons which are emitted with an energy of the order of the eV, but only the latter are considered here. The direction and velocity of secondary electrons emitted by the walls are computed as if they were in thermal equilibrium with a surface at temperature T_s, The statistical distribution in term of directions is therefore not isotropic, and the weight of each direction obeys a cosine law (beside the sine related to solid angle geometry). This raises the following probability densities for the angle with the direction normal to the wall λ, the azimuth Ψ and the energy ε:

$$\begin{aligned} p_\lambda &= \sin\lambda\cos\lambda & \lambda &\in \left[0,\tfrac{\pi}{2}\right] \\ p_\Psi &= \frac{1}{2\pi} & \Psi &\in [-\pi,\pi) \\ p_v &= \frac{\varepsilon}{(kT_s)^2} e^{-\frac{\varepsilon}{kT_s}} & \varepsilon &\in [0,+\infty) \end{aligned}$$

These parameters define the velocity vector of secondary electrons in the close vicinity of the wall, before they are accelerated by the sheath potential.

The stochastic generation of all parameters relies on the usual transformation method, except for ε which is generated by the mean of a rejection method (its probability density is majored by the function $\frac{1}{kT_s} e^{-(1-\frac{1}{e})\frac{\varepsilon}{kT_s}}$ which is easily transformed analytically).

For each type of bulk collision, the free path is determined indirectly through the prescription of a "free volume" defined as

$$V_{free} = \int_0^{\Delta t} \sigma(\varepsilon)\sqrt{\frac{2\varepsilon}{m_e}} \cdot dt$$

where σ is the relevant collision cross-section and Δt the free flight time. It can be shown (e.g. from Eq. 8) that the probability density for V_{free} is:

$$p_{V_{free}} = N_a \cdot e^{-N_a \cdot V_{free}} \qquad V_{free} \in [0,+\infty)$$

The volume $\int_0^t \sigma(\varepsilon)\sqrt{\frac{2\varepsilon}{m_e}} \cdot dt$ generated since the last collision is compared after each displacement to the free volume in order to check whether a collision took place. This method involves the generation of a single random number per collision and is thus faster than a stochastic checking at each step.

Secondary emission is modeled after Sternglass theory of electron secondary emission yield:

$$\delta(\varepsilon) = \delta_m \frac{\varepsilon}{\varepsilon_m} e^{2\left(1-\sqrt{\frac{\varepsilon}{\varepsilon_m}}\right)} \tag{11}$$

taking $\delta_m = 2.9$ and $\varepsilon_m = 600\,eV$, which are typical values for boron nitride [15] and raise a unity yield at $50eV$ consistently with experimental measurements in the low energy range [16].

We make no attempt at determining the sheath potential which is considered as an input of the model. An accurate estimation of the sheath potential as a function of the EEDF was performed by Jolivet and Rousel in[16] and obviously requires a much more sophisticated model. An alternative and simpler approach based on the classical fluid model of sheath proposed in [8] may be used in a later work and could possibly take into account the effect of a space charge limited current through the sheath [17].

4.2 Limitations intrinsic to the numerical method

Besides obvious limitations related to the reduced number of phenomena taken into account, this model cannot be expected in general to give the exact solution of Boltzmann equation. As stated before, the model relies on the uniformity of the plasma which is intrinsically violated by the fact that ionization and attachment at the walls change the net flux of electrons. Except in specific cases, there is no balance between both processes and ionization generally prevails, resulting in an increase of the net current. We believe nevertheless that the results are not too strongly affected by this problem since on one hand attachment partially balances ionization and on the other hand the axial length of ionization is several time the cyclotron radius. A rigorous estimation of the induced perturbation on the EEDF is however lacking at the time of this writing.

4.3 Results

The results of simulations are presented for three different cases, corresponding to three different locations in the channel. Input values are taken from a 1D simulation of the discharge [18] and are summarized in the following table where Φ_w stands for the sheath potential.

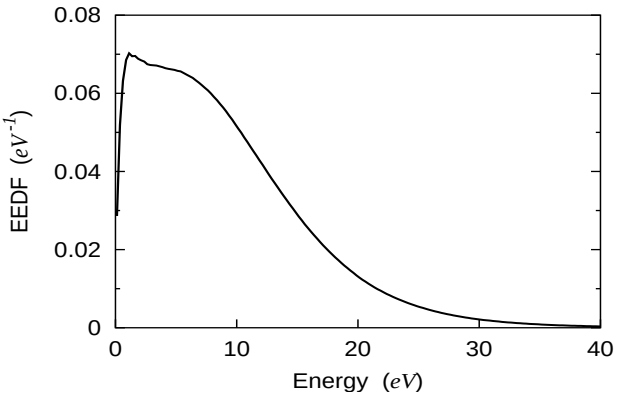

(a) Case 1

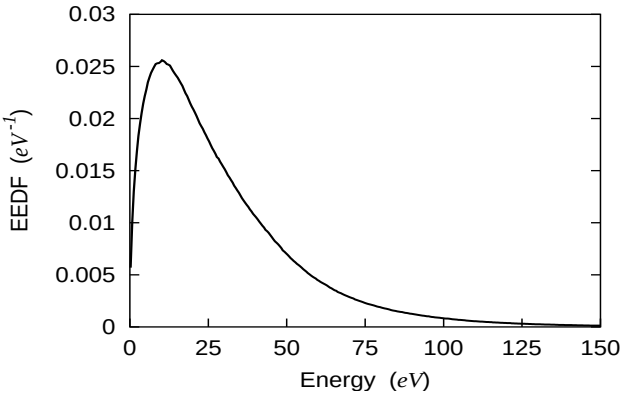

(b) Case 2

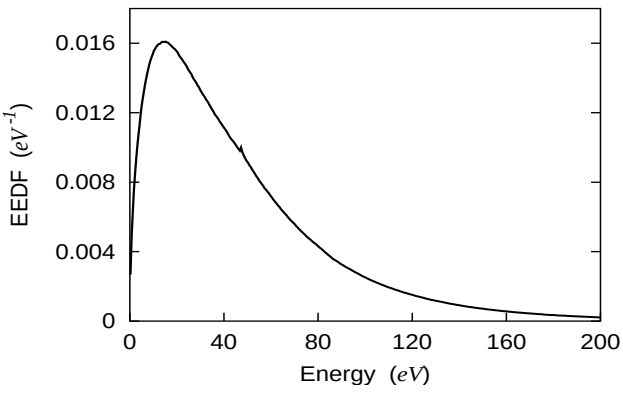

(c) Case 3

Figure 5: Electron energy distribution functions for different plasma and field parameters

Case:	1	2	3
$N_a\ (m^{-3})$	$26\,10^{18}$	$11\,10^{18}$	$6.6\,10^{18}$
$\Phi_w\ (V)$	31	44	47
$B\ (mT)$	6.5	13	17
$E\ (kV.m^{-1})$	3.0	17	30
$\varepsilon_d\ (eV)$	0.61	4.9	8.8

The only significant departure from a Maxwellian distribution can be observed in the first case. The peak at about $2eV$ very likely corresponds to the low bound energy of the cyclotron motion (ε_{min}) for electrons after an inelastic collision. Indeed, the mean energy of electrons in case 1 is rather low, so that most inelastic collisions are performed at energies close to the treshold of inelastic process, thus re-emitting electrons with a very small energy.

One can notice also a small and narrow peak in case 3 at about $50eV$, that is at an energy corresponding to the wall sheath potential. This can be explained by the fact that inelastic collisions with the walls dominate over other inelastic processes at this location in the channel, which results in a large number of secondary electrons being emitted with an energy of the order of the sheath potential.

5 Conclusion

The theoretical possibility of a double hump in the EEDF induced by the peculiarities of the cyclotron motion was confirmed by numerical simulations, at least in the hypothetical case when the dispersion of velocities after inelastic collisions is at most one order of magnitude lower than the drift energy. A more detailed analysis of inelastic processes seem to indicate, however, that such a situation is never met in practice and that the dispersion of post-collision velocity is always comparable or higher than the drift energy.

It is not nonetheless not possible at this point to categorically discard such a possibility since most inelastic processes are too complex to be accurately reproduced in such a simple model. This is for instance the case of excitation processes for which a full collisional-radiative model including the transport of metastable neutrals is theoretically required. Let us mention as well that the reliability of experimental excitation cross-sections is generally very low and difficult to assess.
Similarly, the results were found to strongly depend on the description of wall interactions for which no reliable theoretical model is available in the range of electron energy typical for Hall thrusters. Indeed, there exist very little literature about low energy backscattering, and although there exists several theoretical models of electron secondary emission, none of them has ever been firmly confirmed due to the lack of experimental data in the low energy range.

The present results are consistent with other numerical results [5, 6, 7] which predict a larger departure from the Maxwellian distribution in the low magnetic field region. This contrast with experimental measurements [2] where the departure is larger close to the exit of the channel. Consequently, if the present results can be relied upon for what concerns the qualitative behavior of the EEDF for increasing magnetic field, the presence of a high energy peak in the EEDF cannot be explained on the basis of the energy extrema of the cyclotron motion.

Acknowledgements

This work was performed in the frame of the projects 8-T07A-028-21 and 8-T12D-015-21 funded by the Polish Committee for Scientific Research (KBN) and with the support of Groupement De Recherche CNRS/CNES/SNECMA/ONERA no 2232 « Propulsion à plasma pour systèmes spatiaux ».

References

[1] V. Yu. Fedotov, A. A. Ivanov, G. Guerrini, A. N. Vesselovzrozof, M. Bacal, “On the electron energy distribution function in a Hall thruster”, Physics of Plasma, Vol. 6, No 11, pp. 4360-4365, 1999

[2] G. Guerrini, C. Michaut, M. Dudeck, A. N. Vesselovzorov, M. Bacal, “Characterization of plasma inside the SPT-50 channel by electrostatic probes”, 25th International Electric Propulsion Conference, IEPC 95-053, Cleveland (U.S.A.), August 1995

[3] V. Lago, M. de Graaf, M. Dudeck, “Electron energy distribution function in a stationary plasma thruster plume”, 33rd AIAA/ASME/ SAE/ASEE Joint Propulsion Conference & Exhibit, AIAA Paper 97-3049, Seattle (u.S.A.), July 1997

[4] A. I. Bugrova, A. V. Desiatskov, V. K. Kharchevnikov, A. I. Morozov, “Main features and processes in stationary plasma thrusters”, 23rd International Electric Propulsion Conference, IEPC 93-247, Seattle (U.S.A.), September 1993

[5] L. Garrigues, “Modélisation d’un propulseur à plasma stationnaire pour satellites”, PHD thesis, Paul Sabatier University, Toulouse (France), October 1998

[6] P. Degond, V. Latocha, L. Garrigues, J. P. Boeuf, “Electron transport in stationary plasma thrusters”, Trans. Th. & Stat. Phys. Vol 27, pp-203-221, 1998

[7] V.. Latocha, L. Garrigues, P. Degond, J. P. Boeuf, “Numerical simulation of electron transport in Stationary Plasma Thrusters”, submitted to Plasma Sources Science & Technology

[8] N. B. Meezan, M. A. Cappelli, “Electron Energy Distribution Function in a Hall Discharge Plasma”, 37th AIAA/ASME/ SAE/ASEE Joint Propulsion Conference & Exhibit, AIAA Paper 2001-3326, Salt Lake City, July 2001

[9] E. Passoth, J. F. Behnke, C. Csambal, M. Tichy, P. Kudrna, Yu. B. Golubovskii, I. A. Porokhova, “Radial Behaviour of the Electron Energy Distribution Function in the Cylindrical Magnetron Discharge in Argon”, J. Phys. D: Appl. Phys. Vol 32, p. 2655, 1999

[10] K. Makowski, Z. Peradzyński, S. Barral, M. Dudeck, “Effect of approximate energy balance in Stationary Plasma Thruster”, 36th AIAA/ASME/ SAE/ASEE Joint Propulsion Conference & Exhibit, AIAA Paper 2000-3658, Huntville, Alabama, July 2000

[11] J. A. Syage, “Electron impact cross sections for multiple ionization of xenon and krypton”, Phys. Rev. A 26 no 9, 1992

[12] A. V. Phelps, compilation of collision cross-sections for different gases, available on-line: ftp://jila.colorado.edu

[13] V. Puech, S. Mizzi, “Collision cross-sections and transport parameters in neon and xenon”, J. Phys. D: Appl. Phys. Vol 24, p. 1974, 1991

[14] E. J. Sternglass, “Theory of Secondary Emission”, Westinghouse Lab. Sci. p.1772, 1954

[15] D.C. Joy, “A database on electron-solid interactions”, Scanning vol. 17, pp 270-275 1995

[16] L. Jolivet, J.-F. Roussel, “Effects of the secondary electron emission on the sheath phenomenon in a Hall thruster”, proceedings of the third International Conference on Spacecraft Propulsion, pp. 367-376, Cannes (France), October 2000

[17] G.D. Hobbs, J.A. Wesson “Heat flow through a Langmir sheath in the presence of electron emission”, Plasma Physics, Vol. 9, pp 85-87, 1967

[18] S. Barral, N. Gascon, K. Makowski, Z. Peradzynski, M. Dudeck, “Numerical study of the current-voltage characteristic of Hall thrusters”, 27th International Electric Propulsion Conference, IEPC 01-27, Pasadena (U.S.A.), October 2001